On the accuracy of eikonal approximations in cardiac electrophysiology in the presence of fibrosis

Lia Gander[1], Rolf Krause[1,2][0000−0001−5408−5271], Martin Weiser[3][0000−0002−1071−0044], Francisco Sahli Costabal[4][0000−0002−2612−463X], and Simone Pezzuto[5,1][0000−0002−7432−0424]

[1] Center for Computational Medicine in Cardiology, Euler Institute, Università della Svizzera italiana, Lugano, Switzerland {lia.gander,rolf.krause}@usi.ch
[2] FernUni, Brig, Switzerland
[3] Zuse Institute Berlin, Berlin, Germany weiser@zib.de
[4] Department of Mechanical and Metallurgical Engineering, School of Engineering and Institute for Biological and Medical Engineering, Schools of Engineering, Medicine and Biological Sciences, Pontificia Universidad Católica de Chile, Santiago, Chile fsc@ing.puc.cl
[5] Department of Mathematics, Università di Trento, Povo, Italy simone.pezzuto@unitn.it

Abstract. Fibrotic tissue is one of the main risk factors for cardiac arrhythmias. It is therefore a key component in computational studies. In this work, we compare the monodomain equation to two eikonal models for cardiac electrophysiology in the presence of fibrosis. We show that discontinuities in the conductivity field, due to the presence of fibrosis, introduce a delay in the activation times. The monodomain equation and eikonal-diffusion model correctly capture these delays, contrarily to the classical eikonal equation. Importantly, a coarse space discretization of the monodomain equation amplifies these delays, even after accounting for numerical error in conduction velocity. The numerical discretization may also introduce artificial conduction blocks and hence increase propagation complexity. Therefore, some care is required when comparing eikonal models to the discretized monodomain equation.

Keywords: Cardiac electrophysiology · Fibrosis · Monodomain model · Eikonal model · Eikonal-diffusion model.

1 Introduction

Cardiac arrhythmias, such as atrial fibrillation, are major contributors to morbidity and mortality. Arrhythmias are characterized by a chaotic electrical activity due to re-entrant waves propagating in the cardiac tissue. The risk of occurrence of an arrhythmic event is higher in presence of structural remodeling such as fibrosis, i.e. tissue with altered conductivity and electrophysiological properties. Due to the presence of fibrosis, the conduction velocity in the cardiac tissue is non-homogeneous and the heterogeneity itself is pro-arrhythmic [1].

Computational models of the electrical activity are in use to study arrhythmias and to design treatments. The monodomain model is the most commonly used in *in silico* studies [1–3]. However, the computational demand of the monodomain solution may hinder its applicability in the clinical practice. Eikonal models are a viable alternative in this respect. Eikonal models are approximations of the monodomain model with a much lower computational footprint [4, 5]. These models describe the activation time as a function of space. Here, we consider the eikonal-diffusion equation and the standard eikonal equation. The eikonal-diffusion model is more accurate than the pure eikonal model, as it accounts for curvature effects and heterogeneities [6]. On the other hand, the pure eikonal can be efficiently solved with the Fast Marching or the Fast Iterative method. Moreover, the pure eikonal model is attractive for studying arrhythmias, since its numerical solution can be obtained (with some care) by Dijkstra-like algorithms that allow extensions to describe re-entry [7, 8].

The tissue conductivity plays an important role in the computational models, as it describes the tissue heterogeneity. The conductivity can be discontinuous at the boundaries between the healthy and the fibrotic tissues, for instance. An exemplary situation is shown in the numerical results of Figure 1. In the numerical experiment, we consider a heterogeneous tissue (first panel) and we compare various models for simulating the activation times. As it can be seen, the pure eikonal approximation (fourth panel) noticeably differs from the monodomain approximation (second panel), even after adapting the conduction velocities to minimize numerical errors. Instead, the eikonal-diffusion approximation (third panel) is much more accurate. The discrepancy is due to diffusion currents, not accounted in the pure eikonal formulation. Diffusion currents are due to heterogeneities in the propagation, e.g. curvature, or in the conductivity itself, e.g. discontinuous coefficients.

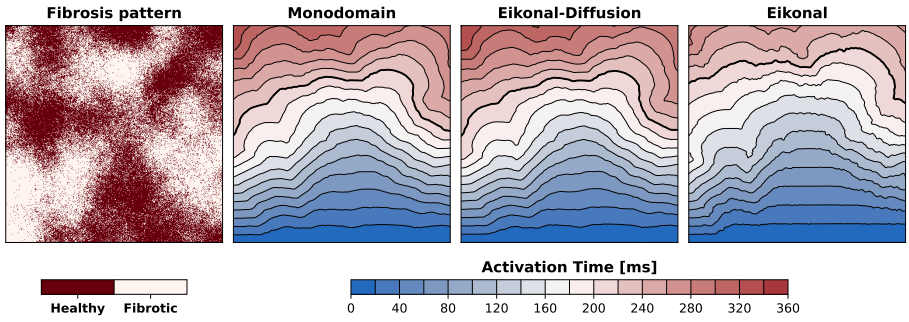

Fig. 1. Comparison between monodomain and eikonal solutions in the presence of fibrosis. The computational domain is a 2-D tissue patch of 15 cm length and height. The spatial resolution in all the models is 0.02 cm. Solutions are reported in terms of isochrones (20 ms spacing). Conduction velocities in the eikonal and eikonal-diffusion model have been adapted to compensate the numerical error in monodomain simulations. The thick contour in the last 3 panels indicates the front position after 220 ms.

In this work, we study the influence of discontinuous conductivity, e.g. due to fibrosis, in the accuracy of the monodomain and the eikonal models. Specifically, we focus on a 1-D fiber, as this enables a precise quantitative assessment of the effect of discontinuities on the overall propagation.

2 Methods

We consider a domain $\Omega \subset \mathbb{R}$ and a time interval $[0, T]$. The monodomain system for the transmembrane potential $v\colon \Omega \times (0,T) \to \mathbb{R}$ reads as follows [6]

$$\begin{cases} \frac{\partial}{\partial x}\left(\sigma(x)\frac{\partial}{\partial x}v(x,t)\right) = \beta\left(C_{\mathrm{m}}\frac{\partial}{\partial t}v(x,t) + I_{\mathrm{ion}}(v,\boldsymbol{y}) - I_{\mathrm{app}}(x,t)\right) & \text{in } \Omega\times(0,T),\\ \frac{\partial}{\partial t}\boldsymbol{y}(x,t) - \boldsymbol{F}(v,\boldsymbol{y}) = 0 & \text{in } \Omega\times(0,T),\\ \frac{\partial}{\partial x}v(x,t) = 0 & \text{in } \partial\Omega\times(0,T),\\ v(x,0) = v_0(x), \quad \boldsymbol{y}(x,0) = \boldsymbol{y}_0(x) & \text{in } \Omega, \end{cases} \tag{1}$$

where $\sigma\colon \Omega \to \mathbb{R}$ is the conductivity, $\beta > 0$ is the surface-to-volume ratio, $C_{\mathrm{m}} > 0$ is the membrane capacitance and $I_{\mathrm{app}}\colon \Omega\times(0,T)\to\mathbb{R}$ is the applied current. Moreover, $\boldsymbol{y}\colon \Omega\times(0,T)\to\mathbb{R}^m$ is a vector of gating and concentration variables of the ionic model determined by the ionic current I_{ion}, the function $\boldsymbol{F}$ and the resting states $v_0\colon \Omega\to\mathbb{R}$ and $\boldsymbol{y}_0\colon \Omega\to\mathbb{R}^m$. In this work we consider the Courtemanche-Ramirez-Nattel ionic model [9] and we set $C_m = 1\ \mu\mathrm{F/cm}^2$ and $\beta = 800\ \mathrm{cm}^{-1}$ [2]. To numerically solve the monodomain equation (1), we consider a mesh with spatial resolution h and the time step Δt. Common choices for the discretization parameters are $h = 0.02$ cm and $\Delta t = 0.01$ ms [2]. For the spatial component, we use a second order finite difference method. For the time integration, we use the first order Euler method for v and the concentration variables and the Rush-Larsen method for the gating variables. We perform the monodomain simulations using the Propag-5 software [10, 11].

The eikonal equations model the activation time $\phi\colon \Omega\to\mathbb{R}$ as a function of the space variable [6]. The eikonal-diffusion equation is

$$\begin{cases} \rho\sqrt{\beta\sigma(x)}\left|\frac{\mathrm{d}}{\mathrm{d}x}\phi(x)\right| - \frac{\mathrm{d}}{\mathrm{d}x}\left(\sigma(x)\frac{\mathrm{d}}{\mathrm{d}x}\phi(x)\right) = C_{\mathrm{m}}\beta & \text{in } \Omega,\\ \frac{\mathrm{d}}{\mathrm{d}x}\phi(x) = 0 & \text{in } \partial\Omega,\\ \phi(x) = 0 & \text{in } \Omega_0, \end{cases} \tag{2}$$

where $\Omega_0 \subset \Omega$ denotes the region where the action potential is initiated and $\rho \in \mathbb{R}$ is a parameter that depends on the ionic model. The parameter ρ represents the velocity of the action potential in an infinite cable with unit surface-to-volume ratio, membrane capacitance and conductivity. It is also the unique solution of the eigenvalue problem

$$\begin{cases} \rho U'(\xi) + \tilde{I}_{\mathrm{ion}}\big(U(\xi)\big) = U''(\xi), & \xi\in\mathbb{R},\\ \tilde{I}_{\mathrm{ion}}\big(U(\xi)\big) \to 0, & \xi\to\pm\infty, \end{cases}$$

where $\tilde{I}_{\mathrm{ion}}$ approximates I_{ion} during the upstroke phase, see [6]. To numerically solve the eikonal-diffusion equation (2), we use the finite element method on a

mesh with resolution h. The non-linearity of the model is handled by a fixed-point iteration on the advection term.

By disregarding the diffusion term in Eq. (2), we obtain the standard eikonal equation, which reads as follows

$$\begin{cases} \rho\sqrt{\sigma(x)}\left|\frac{\mathrm{d}}{\mathrm{d}x}\phi(x)\right| = C_{\mathrm{m}}\sqrt{\beta} & \text{in } \Omega, \\ \phi(x) = 0 & \text{in } \Omega_0. \end{cases} \tag{3}$$

From the eikonal equation it is possible to deduce the formula

$$\mathrm{CV}(x) = \frac{\rho\sqrt{\sigma(x)}}{C_{\mathrm{m}}\sqrt{\beta}} \tag{4}$$

for the conduction velocity $\mathrm{CV}\colon \Omega \to \mathbb{R}$. This observation allows to compute the numerical solution of the eikonal equation (3) on a mesh with resolution h with a simple iterative procedure. Indeed, starting from the nodes in Ω_0, one can compute the activation times in the whole domain Ω by iteratively considering the activation times of the neighbors and the local conduction velocity.

If we assume a constant conductivity σ and we rescale Eq. (2) by the conduction velocity, i.e. if we take $\phi \mapsto \mathrm{CV} \cdot \phi$, we obtain the equation

$$\left|\frac{\mathrm{d}}{\mathrm{d}x}\phi(x)\right| - \varepsilon\frac{\mathrm{d}^2}{\mathrm{d}x^2}\phi(x) = 1, \quad \varepsilon = \frac{\sqrt{\sigma}}{\rho\sqrt{\beta}}. \tag{5}$$

The parameter ε is an estimate of the front thickness. Thus, by Eq. (5), a lower conductivity yields a smaller front, meaning that the front is smaller in fibrotic than in healthy tissue. Moreover, a lower excitability of the membrane (lower ρ) yields a larger front. Note that Eq. (4) and Eq. (5) are still valid in 2-D or 3-D for planar waves.

To model the presence of fibrosis we follow the work of Zahid *et al.* [12]. We consider a reduction of conductivity σ only in the regions where fibrosis is present. In particular, the conductivity is a function of the spatial variable, i.e.

$$\sigma(x) = \begin{cases} \sigma_{\mathrm{h}}, & x \in \text{healthy tissue}, \\ \sigma_{\mathrm{f}}, & x \in \text{fibrotic tissue}, \end{cases}$$

where $\sigma_{\mathrm{f}} < \sigma_{\mathrm{h}}$. We do not account here for the current sink due to fibroblasts, which would be difficult to model with an eikonal approach.

3 Numerical experiments

We perform some 1-D numerical experiments in which an action potential propagates in a tissue line from left to right. In these numerical experiments, we set $\sigma_{\mathrm{h}} = 1.5$ mS/cm [2] and we vary the reduced conductivity σ_{f}.

According to Eq. (4), a reduction in conductivity yields a reduction of conduction velocity, e.g. a 25% reduction in the conductivity corresponds to a reduction to 50% of the conduction velocity. In practice, the conduction velocity

of the monodomain model is affected by a spatial discretization error and does not achieve the conduction velocity of Eq. (4). In particular, the conduction velocity decreases as the spatial resolution h increases, for a finite difference scheme as in this case [13]. This error affects the modeling of the presence of fibrosis, as the predicted reduction in conduction velocity is not achieved. Indeed, at the resolution $h = 0.02$ cm, the conduction velocity in the healthy tissue is 0.0652 cm/ms and the conduction velocity in the fibrotic tissue with $\sigma_f = \sigma_h \cdot 0.25 = 0.375$ mS/cm is 0.0285 cm/ms – less than the expected 0.0652 cm/ms $\cdot$ 0.5 = 0.0326 cm/ms, since the mesh width h relative to front width is larger in fibrotic than in healthy tissue. The discretization error also affects the estimate of the parameter ρ from the monodomain model. A good estimate can be obtained at the fine resolution $h = 0.005$ cm. In this case the monodomain conduction velocity in the healthy tissue is 0.0679 cm/ms, which by Eq. (4) corresponds to $\rho = 1.57$. However, at the resolution $h = 0.02$ cm, the conduction velocities in the healthy tissue and in the fibrotic tissue with $\sigma_f = 0.375$ mS/cm respectively correspond to $\rho_h = 1.51$ and $\rho_f = 1.32$.

We first consider the spatial resolution $h = 0.02$ cm and we focus on the case of $\sigma_f = 0.375$ mS/cm. We perform two numerical experiments in a tissue line of length 15 cm in which we compare the activation times of the monodomain, eikonal-diffusion and pure eikonal models. In the monodomain model the activation time is defined as the time instant when the transmembrane potential v reaches the -62 mV threshold. In the first numerical experiment, the domain consists of a random fibrotic pattern shown at the bottom of Figure 2, panel A, with 62.4% fibrotic tissue. In the plot of Figure 2, panel A, we can see that the activation times of the monodomain model are higher than the activation times of the eikonal-diffusion model, which in turn are slightly higher than the activation times of the pure eikonal model. This can be translated in terms of average conduction velocity, which is 0.0314 cm/ms for the monodomain model, 0.0350 cm/ms for the eikonal-diffusion model and 0.0362 cm/ms for the pure eikonal model. In the second numerical experiment, the domain consists of an

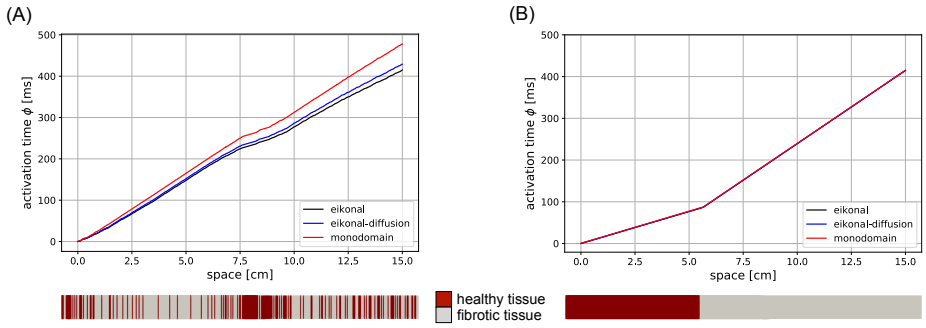

Fig. 2. Activation times in 1-D tissue with a random fibrotic pattern (panel A) and with an ordered fibrotic pattern (panel B).

ordered pattern in which the healthy tissue is on the left and the fibrotic tissue is on the right, see the bottom of Figure 2, panel B. Note that the percentage of fibrotic tissue is the same as in the first numerical experiment. In the plot of Figure 2, panel B, we can see that the activation times of the monodomain, eikonal-diffusion and pure eikonal models are very similar. As a consequence, the average conduction velocity is approximately 0.0362 cm/ms for the three models.

The previous observations suggest that the mismatch between the activation times of the three models is due to the discontinuities in the conductivity σ introduced at the boundaries between the healthy and fibrotic tissue. Indeed, in the first numerical experiment the domain contains 151 discontinuities and the mismatch is significant, whereas in the second numerical experiment the domain contains only one discontinuity and the mismatch is negligible. To further investigate this aspect, we perform a numerical experiment in a domain of length 6 cm consisting of three portions of length 2 cm each. The first and the last portions are healthy tissue, whereas the middle portion is fibrotic tissue. We compare the activation times of the monodomain and eikonal-diffusion models to the activation times of the pure eikonal model. Figure 3 shows the difference in the activation times compared to the pure eikonal model in the case where only two discontinuities are introduced. This plot shows two curves, one for the monodomain model and one for the eikonal-diffusion model. Note that we discard the results in the first and last portions of length 1 cm because they are affected by some boundary effects. Both curves show a negative jump as the action potential propagates from the healthy to the fibrotic tissue and a positive jump as the action potential propagates from the fibrotic to the healthy tissue. In both cases the two jumps are asymmetric, indeed the amplitude of the positive jump

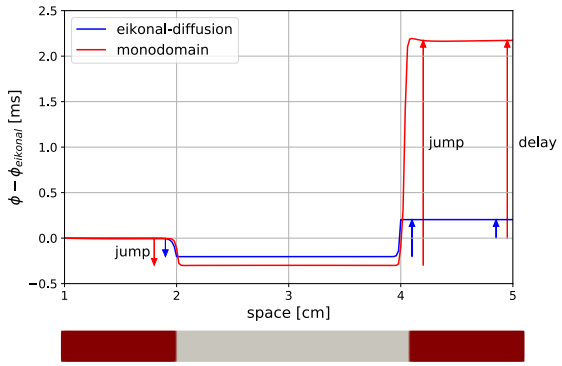

Fig. 3. Difference in the activation times compared to the eikonal model. There is a negative jump when the front propagates from the healthy to the fibrotic tissue and a positive jump when the front propagates from the fibrotic to the healthy tissue. The amplitude of the positive jump is higher than the amplitude of the negative jump. This asymmetry introduces a delay, which is the sum of the two jumps.

is higher than the amplitude of the negative jump. This asymmetry introduces a delay in the monodomain and eikonal-diffusion simulations compared to the eikonal simulations. When the conductivity σ presents many discontinuities, the total delay becomes significant, as in the numerical experiment of Figure 2, panel A. We also observe that the amplitude of the jumps in the monodomain case is higher than the amplitude in the eikonal-diffusion case. This explains why the delay of the monodomain model is more apparent than the delay of the eikonal-diffusion model.

We now consider various spatial resolutions h and different ratios between the fibrotic conductivity σ_{f} and the healthy conductivity σ_{h}. In particular, we study 40 ratios ranging between 0.025 and 1. We consider a domain consisting of two portions with different conductivities. We denote the conductivities on the left and right portions respectively by σ_{left} and σ_{right}. When setting the healthy portion to the left and the fibrotic portion to the right, the ratio $\sigma_{\mathrm{right}}/\sigma_{\mathrm{left}}$ takes our 40 values between 0.025 and 1. Instead, when setting the fibrotic portion to the left and the healthy portion to the right, the ratio $\sigma_{\mathrm{right}}/\sigma_{\mathrm{left}}$ takes 40 values between 1 and 40. For each of these 80 cases, we simulate the propagation with the monodomain and eikonal-diffusion models and we compute the jump of the difference between the resulting activation times and the activation times of the pure eikonal model. The results are plotted in Figure 4, panel A, against $\sqrt{\sigma_{\mathrm{right}}/\sigma_{\mathrm{left}}}$. The plot shows the monodomain curves for the coarse resolution $h = 0.04$ cm, the resolution $h = 0.02$ cm and two fine resolutions $h = 0.01$ cm and $h = 0.005$ cm. The dashed lines are vertical asymptotes that indicate the propagation failure, which occurs with the monodomain model at all resolutions. As $h \to 0$, the monodomain curve converges towards the eikonal-diffusion curve computed with $h = 0.02$ cm, which is a straight line. It is possible to show that, for a wave moving from the left to the right of the discontinuity,

$$\text{jump} \approx \frac{\varepsilon_{\mathrm{right}} - \varepsilon_{\mathrm{left}}}{\mathrm{CV}_{\mathrm{left}}} = \frac{C_{\mathrm{m}}}{\rho^2}\left(\sqrt{\frac{\sigma_{\mathrm{right}}}{\sigma_{\mathrm{left}}}} - 1\right), \tag{6}$$

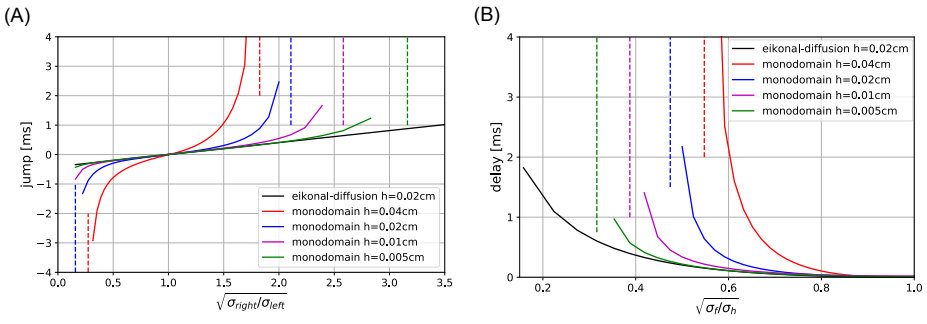

Fig. 4. Panel A: jumps of the difference in the activation times compared to the eikonal model for a front propagating from left to right. Panel B: delay introduced compared to the eikonal model. The dashed lines represent the propagation failure.

where the second equality follows from Eq. (4) and Eq. (5) by assuming that only the conductivity σ is discontinuous. This formula for the jump compares favourably to the numerical values obtained with the eikonal-diffusion model. For example, for the case represented in Figure 3, the formula predicts the jumps -0.19 ms and 0.43 ms, while the numerical values are -0.20 ms and 0.41 ms. Moreover, the formula in Eq. (6) highlights the asymmetry in the jump, i.e. the amplitude of the jump at $\sqrt{\sigma_\mathrm{h}/\sigma_\mathrm{f}}$ is higher than the amplitude at $\sqrt{\sigma_\mathrm{f}/\sigma_\mathrm{h}}$. The delay introduced compared to the pure eikonal model is the sum of the jumps at $\sqrt{\sigma_\mathrm{f}/\sigma_\mathrm{h}}$ and at $\sqrt{\sigma_\mathrm{h}/\sigma_\mathrm{f}}$. These delays are plotted in Figure 4, panel B, against $\sqrt{\sigma_\mathrm{f}/\sigma_\mathrm{h}}$ for the eikonal-diffusion model and the monodomain model at all resolutions h. The dashed lines again illustrate the propagation failure, which always occurs with the monodomain model. Again, there is convergence of the monodomain curve towards the eikonal-diffusion curve as $h \to 0$.

These numerical experiments show that the monodomain results converge towards the eikonal-diffusion results, therefore the eikonal-diffusion model is accurate. The difference between the monodomain and the eikonal-diffusion delays depends on both the spatial resolution h and the value of $\sqrt{\sigma_\mathrm{f}/\sigma_\mathrm{h}}$, see Figure 4, panel B. The pure eikonal model does not capture the delays, therefore the error compared to the eikonal-diffusion model is given by the eikonal-diffusion delays, which depend on $\sqrt{\sigma_\mathrm{f}/\sigma_\mathrm{h}}$, see Figure 4, panel B. The fibrosis model is determined by the value of $\sqrt{\sigma_\mathrm{f}/\sigma_\mathrm{h}}$, which is inversely proportional to the difference between the healthy and fibrotic conduction velocities. Therefore, the accuracy of the monodomain and the pure eikonal models depends on the fibrosis model. Additionally, the accuracy of the monodomain model is also affected by the spatial resolution.

4 Discussion

In this work we show that, in the presence of a high-contrast conductivity, the eikonal-diffusion model matches very well the monodomain solution, in contrast to the pure eikonal model. Indeed, as the spatial resolution tends to zero, the monodomain propagation in 1-D converges towards the eikonal-diffusion propagation. The monodomain model is subject to a numerical error that can significantly affect its outcomes. To guarantee the accuracy of the solutions, the spatial resolution of the monodomain model needs to be selected based on the fibrosis model. However, the choice determined by the fibrosis model might lead to unbearable computational costs. The pure eikonal model does not capture the delays introduced by the discontinuities in the conductivity. As a consequence, the propagation described by the pure eikonal model deviates from the eikonal-diffusion propagation.

Comparisons between eikonal and monodomain have been reported very often in the literature, see e.g. [4, 5] for recent investigations. However, the effect of numerical error on the monodomain equation in the presence of highly heterogeneous conductivity has not been analyzed, to the best of our knowledge. The eikonal-diffusion model has also received little attention, in spite of its very good

accuracy. The main reason is likely the computational cost, since the model is advection-dominated and this may lead to numerical issues at coarse resolutions. Indeed, the local Péclet number of Eq. (2), that is the ratio between the advective and the diffusive term, should be comparable to h^{-1} to ensure a stable solution. In other words, contrary to the pure eikonal model, the mesh requirements of the eikonal-diffusion model are as restrictive as those for the monodomain equation, unless one employs a specific numerical stabilization for the problem. The eikonal-diffusion model can capture boundary and front collision effects, but, more importantly, spatial variations due to conductivity changes. Keener [14] showed that, in the presence of conductivity variation, the conduction velocity is corrected by a term that depends on the derivative of the conductivity. This observation lead to the development of the eikonal-curvature model. A comparison between eikonal-curvature, eikonal-diffusion and pure eikonal has been provided by Pullan *et al.* [15].

This work highlights an important limitation of a pure eikonal approach when modeling cardiac arrhythmias, such as atrial fibrillation or ventricular tachycardia. The accuracy of the pure eikonal model depends on the specific choice of the fibrosis model (pattern, contrast ratio, numerical implementation), thus there is no straightforward way for adapting the conduction velocity so as to match the monodomain propagation. The eikonal-diffusion model is more suitable in this respect, because it guarantees a very good accuracy at a limited computational cost. On the other hand, the pure eikonal model is the ideal starting point in modeling re-entry phenomena [7, 8], with a lot of potential thanks to its very low computational cost. In fact, in spite of the low accuracy in conduction, the pure eikonal model may still match well metrics such as inducibility of arrhythmia [3], thus ensuring its applicability in the clinical context.

Acknowledgments

This work was financially supported by the Theo Rossi di Montelera Foundation, the Metis Foundation Sergio Mantegazza, the Fidinam Foundation, and the Horten Foundation to the Center for CCMC. SP also acknowledges the CSCS-Swiss National Supercomputing Centre (No. s1074). Finally, this work was supported by the European High-Performance Computing Joint Undertaking EuroHPC under grant agreement No. 955495 (MICROCARD) co-funded by the Horizon 2020 programme of the European Union (EU) and the Swiss State Secretariat for Education, Research and Innovation.

References

1. McDowell, K.S., Zahid, S., Vadakkumpadan, F., Blauer, J., MacLeod, R.S., Trayanova, N.A.: Virtual electrophysiological study of atrial fibrillation in fibrotic remodeling. PLoS ONE **10**(2), e0117110 (2015)

2. Gharaviri, A., Bidar, E., Potse, M., Zeemering, S., Verheule, S., Pezzuto, S., Krause, R., Maessen, J.G., Auricchio, A., Schotten, U.: Epicardial fibrosis explains increased endo–epicardial dissociation and epicardial breakthroughs in human atrial fibrillation. Frontiers in Physiology **11**(68), (2020)
3. Gander, L., Pezzuto, S., Gharaviri, A., Krause, R., Perdikaris, P., Sahli Costabal, F.: Fast characterization of inducible regions of atrial fibrillation models with multi-fidelity Gaussian process classification. Frontiers in Physiology **13**, 757159 (2022)
4. Neic, A., Campos, F.O., Prassl, A.J., Niederer, S.A., Bishop, M.J., Vigmond, E.J., Plank, G.: Efficient computation of electrograms and ECGs in human whole heart simulations using a reaction-eikonal model. Journal of Computational Physics **346**, 191–211 (2017)
5. Nagel, C., Barrios Espinosa, C., Gillette, K., Gsell, M.A.F., Sánchez, J., Plank, G., Dössel, O., Loewe, A.: Comparison of propagation models and forward calculation methods on cellular, tissue and organ scale atrial electrophysiology. IEEE Transactions on Biomedical Engineering **70**(2), 511–522 (2023)
6. Colli Franzone, P., Pavarino, L.F., Scacchi, S.: Mathematical cardiac electrophysiology. Volume 13. Springer (2014)
7. Sermesant, M., Konukoglu, E., Delingette, H., Coudière, Y., Chinchapatnam, P., Rhode, K.S., Razavi, R., Ayache, N.: An anisotropic multi-front fast marching method for real-time simulation of cardiac electrophysiology. In: International Conference on Functional Imaging and Modeling of the Heart, 160–169. Springer (2007)
8. Gassa, N., Zemzemi, N., Corrado, C., Coudière, Y.: Spiral waves generation using an eikonal-reaction cardiac electrophysiology model. In: International Conference on Functional Imaging and Modeling of the Heart, 523–530. Springer (2021)
9. Courtemanche, M., Ramirez, R.J., Nattel, S.: Ionic mechanisms underlying human atrial action potential properties: insights from a mathematical model. American Journal of Physiology - Heart and Circulatory Physiology **275**(1), H301–H321 (1998)
10. Potse, M., Dubé, B., Richer, J., Vinet, A., Gulrajani, R.M.: A comparison of monodomain and bidomain reaction-diffusion models for action potential propagation in the human heart. IEEE Transactions on Biomedical Engineering **53**(12), 2425–2435 (2006)
11. Krause, D., Potse, M., Dickopf, T., Krause, R., Auricchio, A., Prinzen, F.: Hybrid parallelization of a large-scale heart model. In: Facing the Multicore - Challenge II, 120–132. Springer (2012)
12. Zahid, S., Cochet, H., Boyle, P.M., Schwarz, E.L., Whyte, K.N., Vigmond, E.J., Dubois, R., Hocini, M., Haïssaguerre, M., Jaïs, P., Trayanova, N.A.: Patient-derived models link re-entrant driver localization in atrial fibrillation to fibrosis spatial pattern. Cardiovascular Research **110**(3), 443–454 (2016)
13. Pezzuto, S., Hake, J., Sundnes, J.: Space-discretization error analysis and stabilization schemes for conduction velocity in cardiac electrophysiology. International Journal for Numerical Methods in Biomedical Engineering **32**(10), e02762 (2016)
14. Keener, J.P.: An eikonal-curvature equation for action potential propagation in myocardium. Journal of Mathematical Biology **29**, 629–651 (1991)
15. Pullan, A.J., Tomlinson, K.A., Hunter, P.J.: A finite element method for an eikonal equation model of myocardial excitation wavefront propagation. SIAM Journal on Applied Mathematics **63**(1), 324–350 (2002)